



This is a repository copy of *Alginate sulfate/ECM composite hydrogel containing electrospun nanofiber with encapsulated human adipose-derived stem cells for cartilage tissue engineering*.

White Rose Research Online URL for this paper:

<https://eprints.whiterose.ac.uk/200114/>

Version: Accepted Version

Article:

Najafi, R., Chahsetareh, H., Pezeshki-Modaress, M. et al. (7 more authors) (2023) Alginate sulfate/ECM composite hydrogel containing electrospun nanofiber with encapsulated human adipose-derived stem cells for cartilage tissue engineering. *International Journal of Biological Macromolecules*, 238. 124098. ISSN 0141-8130

<https://doi.org/10.1016/j.ijbiomac.2023.124098>

Article available under the terms of the CC-BY-NC-ND licence (<https://creativecommons.org/licenses/by-nc-nd/4.0/>).

Reuse

This article is distributed under the terms of the Creative Commons Attribution-NonCommercial-NoDerivs (CC BY-NC-ND) licence. This licence only allows you to download this work and share it with others as long as you credit the authors, but you can't change the article in any way or use it commercially. More information and the full terms of the licence here: <https://creativecommons.org/licenses/>

Takedown

If you consider content in White Rose Research Online to be in breach of UK law, please notify us by emailing eprints@whiterose.ac.uk including the URL of the record and the reason for the withdrawal request.



eprints@whiterose.ac.uk
<https://eprints.whiterose.ac.uk/>

Alginate sulfate/ECM composite hydrogel containing electrospun nanofiber with encapsulated human adipose-derived stem cells for cartilage tissue engineering

Roghayeh Najafi^{1,&}, Hadi Chahsetareh^{1,&}, Mohamad Pezeshki-Modaress², Mina Aleemardani³, Sara Simorgh^{4,5}, Seyed Mohammad Davachi⁶, Rafieh Alizadeh⁷, Alimohamad Asghari⁸, Sajad Hassanzadeh^{8,9**}, Zohreh Bagher^{7,5,*}

¹ Department of Life Science Engineering, Faculty of New Science and Technologies, University of Tehran, Iran.

² Burn Research Center, Iran University of Medical Sciences, Tehran, Iran

³ Biomaterials and Tissue Engineering Group, Department of Materials Science and Engineering, Kroto Research Institute, The University of Sheffield, Sheffield S3 7HQ, UK

⁴ Cellular and Molecular Research Center, Iran University of Medical Sciences, Tehran, Iran.

⁵ Department of Tissue Engineering and Regenerative Medicine, Faculty of Advanced Technologies in Medicine, Iran University of Medical Sciences, Tehran, Iran

⁶ Department of Biology and Chemistry, Texas A&M International University, Laredo, TX 78041, USA.

⁷ ENT and Head and Neck Research Center and Department, The Five Senses Health Institute, School of Medicine, Iran University of Medical Sciences, Tehran, Iran

⁸ Skull Base Research Center, The Five Senses Health Institute, School of Medicine, Iran University of Medical Sciences, Tehran, Iran

⁹ Eye Research Center, The Five Senses Health Institute, School of Medicine, Iran University of Medical Sciences, Tehran, Iran

& R. Najafi and H. Chahsetareh contributed equally to this work.

*Corresponding author: Z. Bagher, E-mail: bagher.z@iums.ac.ir

**Corresponding author: S. Hassanzadeh, E-mail: hassanzadeh.sa@iums.ac.ir

Abstract

Stem cell therapy is a promising strategy for cartilage tissue engineering, and in recent studies, cell transplantation through polymeric scaffolds has gained attention. Herein, we encapsulated human adipose-derived stem cells (hASCs) within the alginate sulfate hydrogel, and for the betterment of mimicking the cartilage structure and characteristic, polycaprolactone/gelatin electrospun nanofibers, and extracellular matrix (ECM) powder have been added. The composite hydrogel scaffolds were developed to evaluate the relevant factors and conditions in mechanical properties, cell proliferation, and differentiation to enhance cartilage regeneration. To this aim, initially, different concentrations (1-5% w/v) of ECM powder were loaded within an alginate sulfate solution to optimize the best composition for encapsulated hASCs viability. The results revealed that ECM addition significantly improved mechanical properties and cell viability, and 4% w/v ECM was chosen as the optimum sample. At the next step, electrospun nanofibrous layers were added to the alginate sulfate/ECM composite to prepare different layered hydrogel-nanofiber (2, 3 and 5-layer) structures with the ability to mimic the cartilage structure and function. 3-layer was selected as the optimum layered composite scaffold, considering cell viability, mechanical properties, swelling and biodegradation behavior; moreover, the chondrogenesis potential was assessed and the results showed promising features for cartilage tissue engineering application.

Keywords: Alginate sulfate; Stem cells; Cartilage tissue engineering; Composite scaffolds; Hydrogel/nanofiber

1. Introduction

Cartilage is an avascular, aneural, alymphatic, resilient, and smooth elastic connective tissue, which is composed of chondrocyte cells, mainly located at the ends of the bones, where joints are located. There are three types of cartilage, hyaline (the most abundant type), fibrous, and elastic in the human body [1,2]. Cartilage can be damaged by different factors such as osteoarthritis, inflammatory arthropathies, cartilaginous tumors, chondrocalcinosis, relapsing polychondritis, osteochondritis, dissecan, trauma, spondyloepimetaphyseal dysplasia (SEMD), and ageing. Unfortunately, so far, there is no optimal treatment for cartilage damage since the cause and pathogenesis of cartilage diseases are not fully understood [2–4]. One of the difficulties of this field is that until the degradation of extracellular matrix (ECM) components, no symptoms are seen because cartilage has no neurons, making the cartilage treatment so challenging. However, there are several methods used to treat cartilage damage, containing microfracture, mosaicplasty, autologous chondrocyte implantation (ACI) [5], and novel biomedical techniques (e.g., stem cell therapy and tissue engineering). Although these techniques can be used as treatments, still, there are some challenges, such as not fully understanding cartilage aetiology and pathogenesis, lags of diagnosis due to the aneural nature of the tissue, and difficulties of drug and biomolecule delivery because of being avascular [2,6,7]. Tissue engineering (TE) with a combination of cell, scaffold, and signaling (mechanical, chemical, and electrical signals) offers a promising approach for the regeneration of cartilage that can overcome the present issues [8,9].

Lately, using stem cells to treat various diseases and disorders has gained much attention; it can be said it is because of the two significant features: being self-renewable and the ability to differentiate into a specialized adult cell type. Subcutaneous and omental fat tissues are suitable sources of these stem cells because of their abundance and availability. It is possible for the stem

cells that originated from fat cells to differentiate into fat tissue, osteogenic, chondrogenic, mesenchymal lineages, and other tissues. By supplying the condition for these stem cells to be differentiated into chondrocytes, they can be utilized for injured joints, Arthritis, or joint recuperation [10–13]. For instance, Tsai et al. evaluated encapsulated human adipose-derived stem cells (hASCs) within enzyme-cross-linked gelatin hydrogel for hyaline cartilage regeneration in rabbits. In vitro and in vivo studies demonstrated that the encapsulated stem cells had high proliferation and chondrogenic differentiation potential in the hydrogel [14].

The ECM plays a significant role in cartilage function, and generally, it provides a microenvironment network for cells to determine cell fate and maintain the cellular phenotype. In each tissue, the topology and composition of ECM are different; therefore, decellularization of cartilage tissue and the use of ECM powder can help construct ECM closer to the native one, which allows cells to behave similarly to the cells within the native ECM. Decellularized ECM (dECM) can be prepared from human and animal sources and with a variety of methods like mechanical, chemical, and enzymatic [15]. Rothrauff et al. decellularized cartilage tissue with the chemical method and almost no trace of the DNA (99%) in the cartilage [16]. In comparison, Oh et al. decellularized porcine cartilage tissue with the mechanical method and removed 98% of the DNA in the cartilage [17].

Hydrogels are one of the most potential three-dimensional (3D) scaffolds used in TE to deliver drugs, growth factors, and cells. The hydrogel structure allows for mimicking the native ECM (ref); thus, it is a suitable microenvironment for cell adhesion, proliferation, and differentiation. Another type of scaffold that is well-known for providing ECM-like structure is electrospun nano or microfibers [18]. The idea of laminated composites, entailing layer-by-layer fibers and hydrogels, enables a high percentage of mimicking ECM, improving mechanical

strength and controllable degradation time and rate. A wide range of natural and synthetic biopolymers in various forms of scaffolds (e.g., hydrogel, sponge, and mesh) are used for cartilage regeneration [4]. Natural biopolymers like collagen, gelatin, silk fibroin, chitosan, hyaluronic acid, alginate, bacterial cellulose, dextran, and polyhydroxyalkanoate have suitable biological properties; on the other hand, still, there are some challenges related to supplying appropriate mechanical properties resemble cartilage that limits their effective use. Synthetic biopolymers such as poly(ϵ -caprolactone) (PCL), polyurethane, polypropylene fumarate, polyphosphazene, poly(1,4-butylene succinate), poly(lactic-co-glycolic acid) (PLGA), and polylactic acid (PLA) present proper mechanical properties, higher than natural polymers; although, they have poor biological properties [19,20]. Hybrid scaffolds made of natural and synthetic biomaterials have indicated several advantages, which outweigh the limitations of singular usage [21].

PCL can be named a representative of synthetic biopolymers, an aliphatic linear polyester with a wide molecular weight (from 3000 – 100,000 g.mol⁻¹), with slow degradability (2–4 years), high mechanical properties, poor biocompatibility, and FDA approval. Gelatin (GT), a highly applicable natural biopolymer obtained from the hydrolysis of collagen, has fine gel strength, high biocompatibility, fast biodegradability, and poor mechanical properties [22–24]. PCL/GT electrospun has been widely investigated in different fields of TE like skin, nerve, dental, cardiovascular, and muscle [25]. For instance, Zheng et al. evaluated various blend ratios of PCL/GT to produce electrospun nanofibers for the 3D construct shape of cartilage. Evaluation of cell attachment and proliferation of chondrocytes demonstrated that all the scaffolds have proper biocompatibility and PCL/GT 30:70 was suitable for fabricating ear-shaped cartilage [25].

Alginate is a linear natural biopolymer derived from the cell walls of brown algae. The G-blocks and M-blocks of the alginate determined physicochemical properties such as viscosity and

water uptake ability. Alginate hydrogel can be prepared by combining the solution with ionic cross-linking like divalent cations (e.g., Ca^{2+} , calcium chloride is the most common one) [26,27]. It has been shown that encapsulated chondrocytes within alginate hydrogels are capable candidates for cartilage and bone tissue engineering [20]. Alginate can be converted to alginate sulfate by several methods; the sulfate group in alginate sulfate is one of the important components in native ECM. Therefore, sulfate alginate creates a suitable environment for the proliferation and migration of cells by providing a more ECM-like environment [28].

In this study, to better mimic the cartilage, various factors that are effective for cartilage regeneration have been gathered together, and composite scaffolds made of hydrogels and nanofibers have been developed. The usage of hydrogels and nanofibers helps mimic the cartilage structure, while the influence of the number of composite layers (hydrogels and nanofibers) has been examined and optimized. The main novelty of the current work is the encapsulation of hASCs in the composite hydrogel containing ECM powder, which biologically and mechanically resembles the native cartilage. Moreover, to the best of our knowledge, the investigation of the effects of the nominal percentage of ECM in hydrogel on stem cell behavior and the number of composite layers on stem cell behavior and mechanical properties are investigated for the first time. In this regard, hASCs were encapsulated within sodium alginate and alginate sulfate hydrogel with different concentrations of ECM powder (0-5% w/v) to determine the optimal concentration of ECM based on the cell viability and mechanical behavior. Then, to fabricate the laminated composite scaffold, the scaffold was constructed with several different layers of PCL/GT nanofibers and hydrogels containing the optimal ECM powder. Finally, the prepared scaffolds have been analyzed by conducting multiple assays to examine physicochemical and biological characteristics.

2. Materials and methods

2.1. Materials

Polycaprolactone (PCL), Gelatin type A (GT), acetic acid (AA, >99.85%), formic acid (FA), calcium chloride-dihydrate (CaCl_2), alginate sulfate, sodium alginate (200–300 kDa MW), phosphate-buffered saline (PBS), collagenase type 1, penicillin, sodium dodecyl sulfate (SDS), ethylenediaminetetraacetic acid (EDTA, Merck), deoxyribonuclease (DNase, 500U, Sinaclon, Iran), sodium chloride-Tris-EDTA, phenol, chloroform, isoamyl alcohol, formaldehyde, and streptomycin were purchased from Sigma Aldrich (St. Louis, MO). Dulbecco's Modified Eagle Medium/Nutrient Mixture F-12 (DMEM/ F12) and fetal bovine serum (FBS) were obtained from Gibco.

2.2. Synthesis and characterization of electrospun nanofiber

For the electrospinning solution, PCL and GT with a concentration of 15% w/v were separately dissolved in AA/FA (90:10) at room temperature and then mixed with the blend ratio of 70:30 to achieve the total polymer concentration of 15% w/v [29]. After preparing the precursor, it was shed in a plastic syringe, and the nanofibers were prepared by electrospinning (voltage 20 kV, feed rate 1 ml/h, 14 cm distance, and drum speed 50 rpm). The residual solvent of the PCL/GT nanofibers was evaporated in a vacuum oven (48 h, 50 °C). The fiber diameter and morphology of electrospun nanofiber were investigated by scanning electron microscopy (Zeiss, Germany). Electrospun nanofibers before imaging were coated with gold by using sputtering apparatus. About 100 nanofibers were randomly analyzed using image analysis software (Image J 1.42q).

2.3. Decellularization of bovine hyaline cartilage, DNA content, and histological analysis

After sacrificing the calf, hyaline cartilage was harvested from femoral condyles and freshly cut into smaller pieces with a surgical blade and then washed with PBS [15–17]. Firstly, the minced cartilages were placed in SDS (1% w/v) and PBS solution for 72 h with stirring at 300 rpm at room temperature to denature proteins and cell lysis (every 24 h refreshed the solution). Then the tissue was soaked in EDTA (0.01% w/v) and PBS solution, stirring at 300 rpm for 24 h. After that, it was treated with deionized water for 24 h to remove all organic solvents (every 8 h refreshed the solution). The washed pieces were digested in 10 ml PBS containing 10 μ l DNase for 2 h and washed with PBS for 24 h. Afterwards, acellular hyaline cartilage was lyophilized and made into a fine powder with a mixer mill.

DNA content was investigated to be sure of the decellularization process; decellularized samples (Decell: 0.1366 g) with bovine hyaline cartilage as control (0.1339 g) were placed in a digestion buffer containing SDS, STE buffer, and proteinase K enzyme. The separation process was performed in two stages with phenol/chloroform/isoamyl alcohol (1/24/25), and DNA precipitation was performed with ethanol 100%. Finally, the DNA was dissolved in 50 μ l of sterilized distilled water. The Decell was centrifuged (10000 G and 10 min) and was measured the absorbance of the top layer containing DNA at 260 nm (Thermo Fisher, Spectrophotometers, NanoDrop™ 2000/2000c).

The decellularized tissue and native tissue were fixed in 10% formaldehyde (10% v/v) for 24 h and then dehydrated, and after that embedded in paraffin wax. The Decell, after cutting by microtome and placing onto glass slides, dewaxed and then were stained with hematoxylin-eosin (H&E) to determine the decellularization rate.

2.4. Preparation of hydrogels

Hydrogel solutions with the concentration of 2% w/v of alginate and alginate sulfate (50:50) and different concentrations of ECM powder (0%, 1%, 2%, 3%, 4 and 5% w/v) in PBS at room temperature (**Figure 1A**) were prepared [30].

2.5. Fourier transform infrared spectroscopy (FTIR)

The chemical structure of the alginate and alginate sulfate hydrogel with ECM powder (4% w/v; optimal sample) was determined by Fourier transform infrared (FTIR) analysis. The hydrogel without ECM was also analyzed as the control group. Spectra were collected from 400 to 4000 cm^{-1} , 4 cm^{-1} resolution, 16 scans using a spectrometer (PerkinElmer Co. US).

2.6. hASCs cells culture and encapsulation in hydrogels

hASCs were isolated from human adipose, as previously explained (**Figure 1A**). Briefly, human adipose biopsies were isolated using collagenase (0.5%), and after that, incubated in DMEM/ F12 medium supplemented with penicillin-streptomycin (1%) and FBS (10%) at 37 °C and 5% CO₂. The culture medium was changed every other day. The third-passage cells were used for further assessment. hASCs were evaluated using a BD FACS Calibur instrument (BD Biosciences, San Jose, CA, USA) with the Flow Jo software for cell surface markers containing CD 29, CD 31, CD 34, CD 90, and CD 105. hASCs were encapsulated in the hydrogel with different concentrations of ECM powder [30]. Briefly, firstly, sterilization of alginate and the alginate sulfate powder (1 h), the alginate/alginate sulfate solutions with various concentrations of ECM are constructed, as explained previously. Secondly, 1×10^4 cells of hASCs (20 μl) were combined with 20 μl of hydrogel solutions in a 96-cell culture plate. Then, hydrogel solutions were crosslinked with 100 μl of CaCl₂ (1% w/v) for 10 min. After that, 150 μl medium (DMEM/F12, 10% FBS and 1% penicillin-streptomycin) was added to each well, and it was refreshed every day.

The hydrogel without ECM powder, the hydrogel with 1, 2, 3, 4 and 5% w/v ECM powder groups were investigated.

2.7. Preparation of laminated composite scaffolds

To prepare laminated composite scaffolds (**Figure 1B**): (1) the 2-layer, electrospun fibers were punched with 9 mm diameter and put in 48 well plates, and hydrogel solution was poured on them [31], (2) the 3-layer scaffold, the punched electrospun fibers put in 48 well cell culture plate, and hydrogel solution was poured on them, and then the electrospun fibers were added and (3) the 5-layer scaffold consists of 2-layer of hydrogels and 3-layer of electrospun fibers, which is stacked on top of each other. All the scaffolds were crosslinked with CaCl_2 (1% w/v) for 10 min at 37 °C.

2.8. Cell encapsulation in laminated composite scaffolds

Within the hydrogel layer(s) of composite scaffolds, hASCs were encapsulated [32]. Briefly, the multi-layer scaffold of hydrogel with ECM powder (4% w/v) and electrospun nanofibers was made, as mentioned previously. In this regard, 1×10^4 cells of hASCs (20 μl) were combined with 20 μl of hydrogel solutions and then poured on nanofiber in a cell culture plate. Then, laminated constructs (2-layer, 3-layer, and 5-layer) were crosslinked with 100 μl of CaCl_2 for 10 min. Finally, 150 μl medium (DMEM/F12, 10% FBS and 1% penicillin-streptomycin) was added to each well and it was refreshed every day. 2-layer, 3-layer, and 5-layer groups of laminated composite scaffolds were investigated.

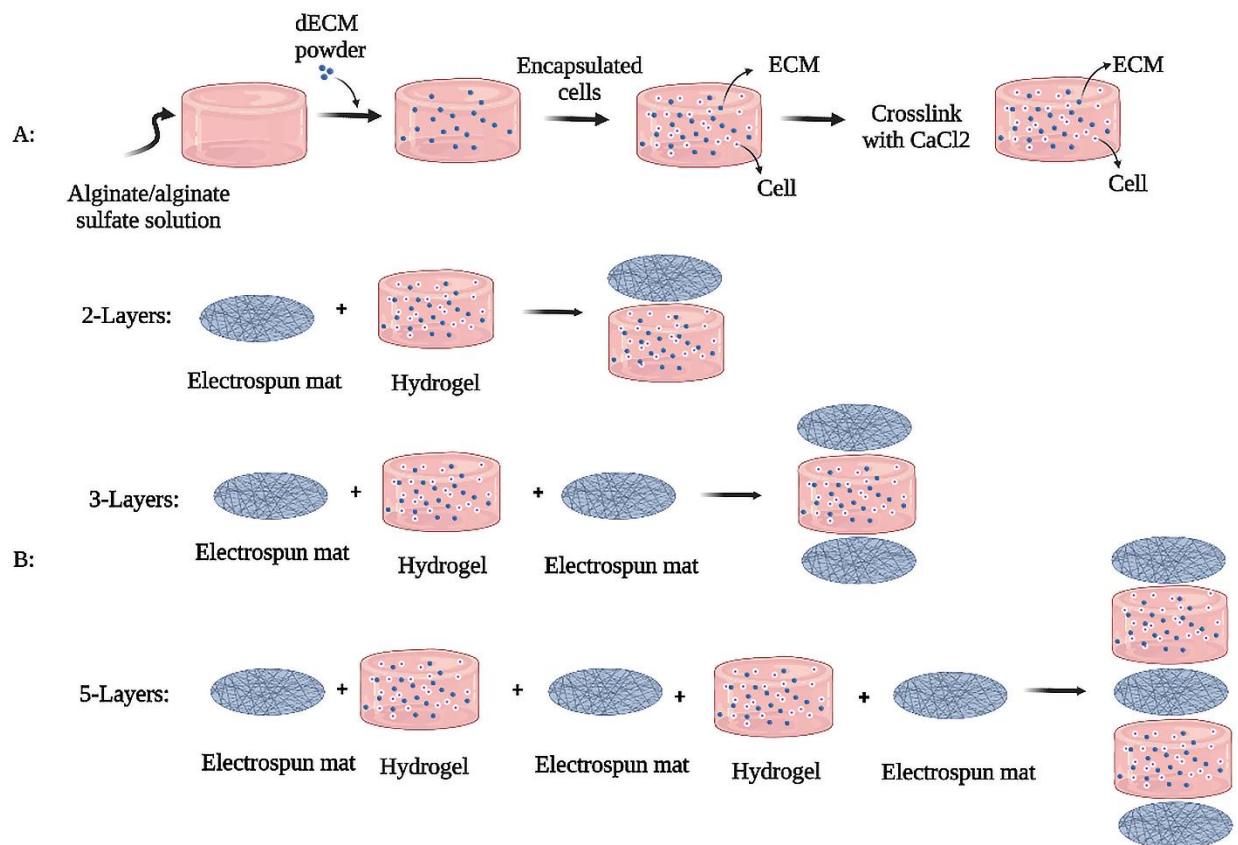


Figure 1. Schematic of preparing (A) hydrogel containing ECM and cell and (B) laminated composite scaffolds: 2-layer, 3-layer scaffold, 5-layer. All the scaffolds were crosslinked with CaCl₂.

2.9. Water retention ability

The water retention ability of the composites was investigated by immersing samples in PBS with pH 7.4 at 37 °C for 24 h [33,34]. Considering the composite initial and after soaking weights to be W_d and W_w , the water uptake capacity was described as the increase of weight ratio after soaking ($W_w - W_d$) to the initial weight (W_d) (Eq. 1). The values are expressed as the mean \pm standard error ($n = 3$).

$$W = [(W_w - W_d) / (W_d)] \times 100 \quad (1)$$

2.10. Biodegradation

The PBS solution with pH 7.4 at 37 °C was used as the simulated degradation environment of the human body for the degradation of the laminated composite scaffolds [33,34]. After weighing the composites, they were placed into 24-well plate with 1 ml of PBS and incubated at 37 °C for 1, 3, 7, 14, and 21 days. After the intended period for biodegradation, all the composites were soaked in deionized water and then dried and weighed. Degradation rates were calculated from the dried weight of the scaffold before (W_{d1}) and after soaking (W_{d2}) in PBS. The values are expressed as the mean \pm standard error ($n = 3$).

$$W = [(W_{d1} - W_{d2}) / (W_{d1})] \times 100 \quad (2)$$

2.11. Mechanical properties

The mechanical property of cylindrical samples (8 mm diameter and a height of 10 mm) was determined by a mechanical analyzer (SANTAM, STM-20) [35]. For the unconfined compressive strength, Young's modulus of specimens was evaluated using a 6N load with a 2.5 mm/min rate at room temperature. The compressive-strain cycle was performed load corresponding to a 60% strain level and in the condition of a 6 N load with a rate of 2.5 mm/min at room temperature. The values are expressed as the mean \pm standard error ($n=3$).

2.12. Rheological properties of the hydrogels

The rheological properties of the hydrogels were conducted at 37 °C using Anton Paar Physica MCR300 rheometer (Graz, Austria) equipped with a cone and plate CP25 geometry according to ASTM D4440 under air atmosphere to find out the optimized ECM content. The dynamic experiments were measured under oscillatory shear mode with hydrogel sample under cone and plates. Frequency sweep experiments were performed over the frequency range of 0.01–100 Hz, and the elastic modulus (G'), loss modulus (G''), and complex viscosity were obtained.

Prior to the frequency sweep measurement, the strain was optimized using amplitude sweep experiments to stay in the linear viscoelastic region.

2.13. Cell viability (MTT) assay

Cell viability of hASCs was determined quantitatively by 3-(4,5-dimethylthiazol-2-yl)-2,5-diphenyl-2H-tetrazolium bromide (MTT) (Kiazist, Tehran, Iran) [36]. At the intended time, the culture medium was removed with PBS, and then 150 μ l of fresh medium (FBS free) with 20 μ l of the MTT assay reagent was added to each well and incubated (37 °C and 5% CO₂) for 4 h. After that, the solubilizer (DMSO, 100 μ l) was added to the well plate, and the ELISA plate reader at 570 nm measured the absorption.

2.14. Chondrogenic differentiation and Alcian Blue stain analysis

The chondrogenic differentiation of hASCs was analyzed by applying an Alcian Blue stain after 21 days [37,38]. 2×10^5 hASCs (fourth passages) were encapsulated in the hydrogel layer of prepared composite sandwich constructs. The composite containing hASCs was incubated under high humidity for 2 h, and chondrogenesis media (StemPro, Gibco; Invitrogen, Grand Island, NY) was added to the 12-well cell culture plate and incubated (37 °C and 5% CO₂). Then the composites were dehydrated, fixated, embedded in paraffin wax, and sliced into sections with 5 μ m thickness by microtome. The samples were placed onto glass slides and stained with 1% Alcian Blue. The rate of synthesis of proteoglycans was qualitatively investigated by light microscopy.

2.15. Real-time PCR

The chondrogenic differentiation of hASCs was analyzed by applying a real-time PCR after 21 days. For this purpose, 5×10^5 hASCs (fourth passages) were encapsulated in the hydrogel layer of composite sandwich constructs. The composite containing hASCs was incubated under high humidity for 2 h, and chondrogenesis media (StemPro, Gibco; Invitrogen, Grand Island, NY)

was added to the 12-well cell culture plate and incubated (37 °C and 5% CO₂). Following manufacturer guidelines, the total RNA was extracted from the hASCs growing inside the hydrogel layer and on the TCP group through RNX-Plus (Sina Clon, Tehran, Iran). After that, total RNA was extracted using a cDNA synthesis kit (Takara, Shiga Prefecture, Japan), and oligo primers were transformed into cDNA. Then cDNA was stained with Eva Green master mix, and real-time PCR analysis was done by the real-time PCR analyzer (Corbett, Mortlake, Australia) for a 45 cycle. The expression levels of each gene such as collagen II (COL II), SRY-Box Transcription Factor 9 (SOX 9), and Aggrecan (ACAN) were calculated by the $2^{-(\Delta\Delta CT)}$ method (beta Actin (β -actin) used as a control marker). The gene primer sequences used in the real-time PCR are outlined in Table 1.

Table 1. primers sequences utilized for real-time PCR

Target Gene	Primer sequence (5'–3')
COL II	GCC AAG GGT CTG ACT CCC ATC ACA CCA GCC
SOX9	GCA GGA GGA GAA GAG AA GAG GCG AAT TGG AGA GGA
ACAN	TGT CAG ATA CCC CAT CC CAT AAA AGA CCT CAC CCT
β -actin	CTT CCT TCC TGG GCA T GTC TTT GCG GAT GTC C

2.16. Statistical analysis

Statistical analyses were performed using Origin software (2021). Two-way ANOVA statistical tests were used. Results with a p-value of less than 0.05 were considered significant.

3. Results and discussion

3.1. Characterization of electrospun nanofibers

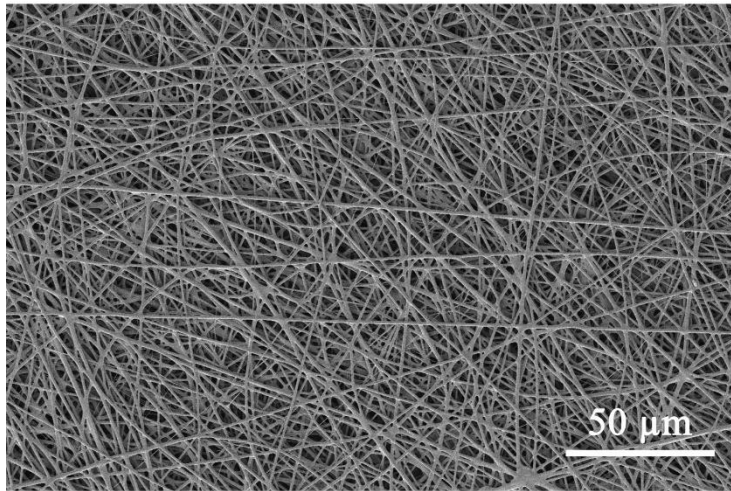
Electrospinning was used to create nanofibers, and by SEM, the morphology and distribution of electrospun fibers were characterized. The SEM result (**Figure 2A**) showed that the nanofibers have a random orientation and smooth surface without beads with an average diameter of 124.7 ± 14 nm. The native ECM contains nano and microfibers; as shown in **Figure 2B**, the fabricated electrospun mat can mimic ECM. The formation of micro and nanofibers is due to the phase separation of PCL and GT in the electrospinning solution [39].

3.2. Characterization of decellularized cartilage ECM

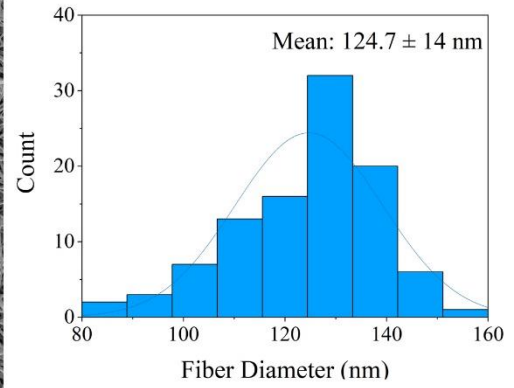
The ECM powder provides a tissue-like structure containing growth factors and is one of the widely used biomaterials as a scaffold. Mainly, the animal or human ECM is utilized as the scaffold, which is suitable for maintaining tissue shape, culture medium, and injectable scaffolds [15]; therefore, it has been chosen as one of the components of the designed scaffold. DNA content and H&E staining were performed to ensure the effectiveness of the decellularization efficiency technique. The results of the DNA content assay (**Figure 2C**) demonstrated that the amount of native tissue DNA was 192.4 ng/ μ l, which was reduced to 45.2 ng/ μ l following decellularization. Thus, it presents the success of this method which is consistent with other studies. **Figure 2D** and **2E** illustrate the H&E images, showing a well-preserved architecture of the collagen, and keeping the cytoplasmic and ECM components in a homogeneous pattern. Collagen fibers were seen in histological staining as pink and had a particular order in this connective tissue. Three zones of each group were selected for semi-quantification evaluation of H&E images, and in each zone, the cells that remained intact were counted by ImageJ (1.52v). The assessment of the nuclear count

stained with H&E showed that the cell number in the decellularization matrix compared with native tissue decreased significantly. Results obtained from H&E of native and decellularization matrix depicted similar results as those achieved with DNA content.

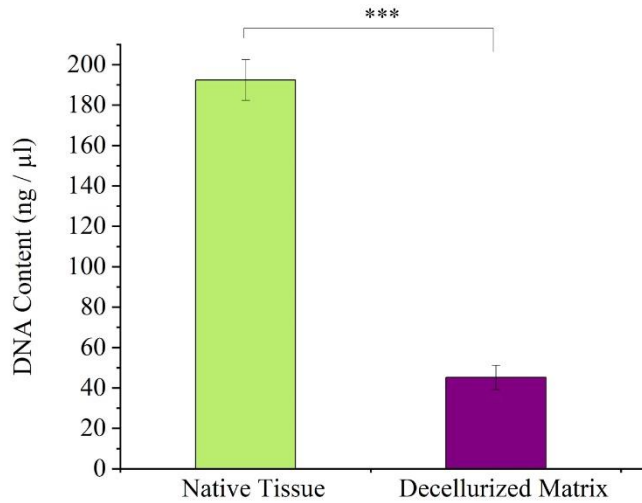
A



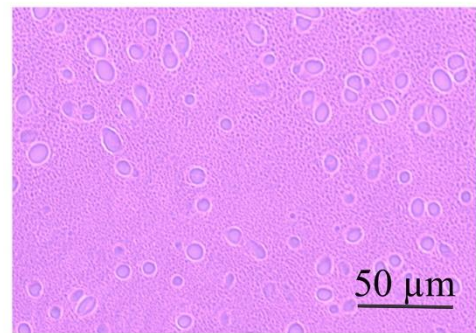
B



C



D



E

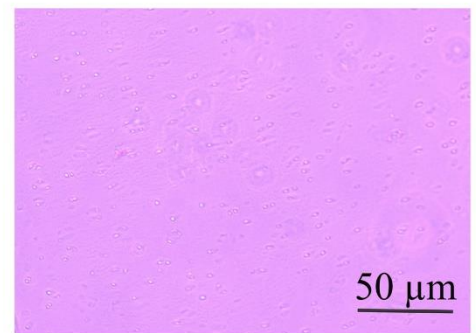


Figure 2. (A) Structure and morphology of PCL/GT nanofibers, (B) the histogram of fiber diameter distribution of nanofibers (mean = 124.7 ± 14 nm), (C) DNA content for native tissue and decellularized matrix (n = 3; ***p < 0.0005), H&E staining of (D) decellularized matrix and (E) native tissue.

3.3. Fourier transform infrared spectroscopy (FTIR)

Figure 3 illustrates the FTIR spectrum of the hydrogel with and without ECM. The FTIR spectra of sodium alginate showed a large absorption band in the range of $3600 - 3000 \text{ cm}^{-1}$ due to the stretching vibration band of the OH group and the -CH vibration bands at $2930 - 2845 \text{ cm}^{-1}$ [40]. The peak at nearly 1250 cm^{-1} is assigned to S=O symmetric stretching indicating sulfation of the uronic acids in alginate [41]. FTIR spectra of the cartilage ECM (4% w/v) revealed typical amide bands at 1655 , 1338 , and 1240 cm^{-1} , indicating C=O stretching (Amide I), N-H deformation (Amide II), and N- deformation (Amide III), respectively [42].

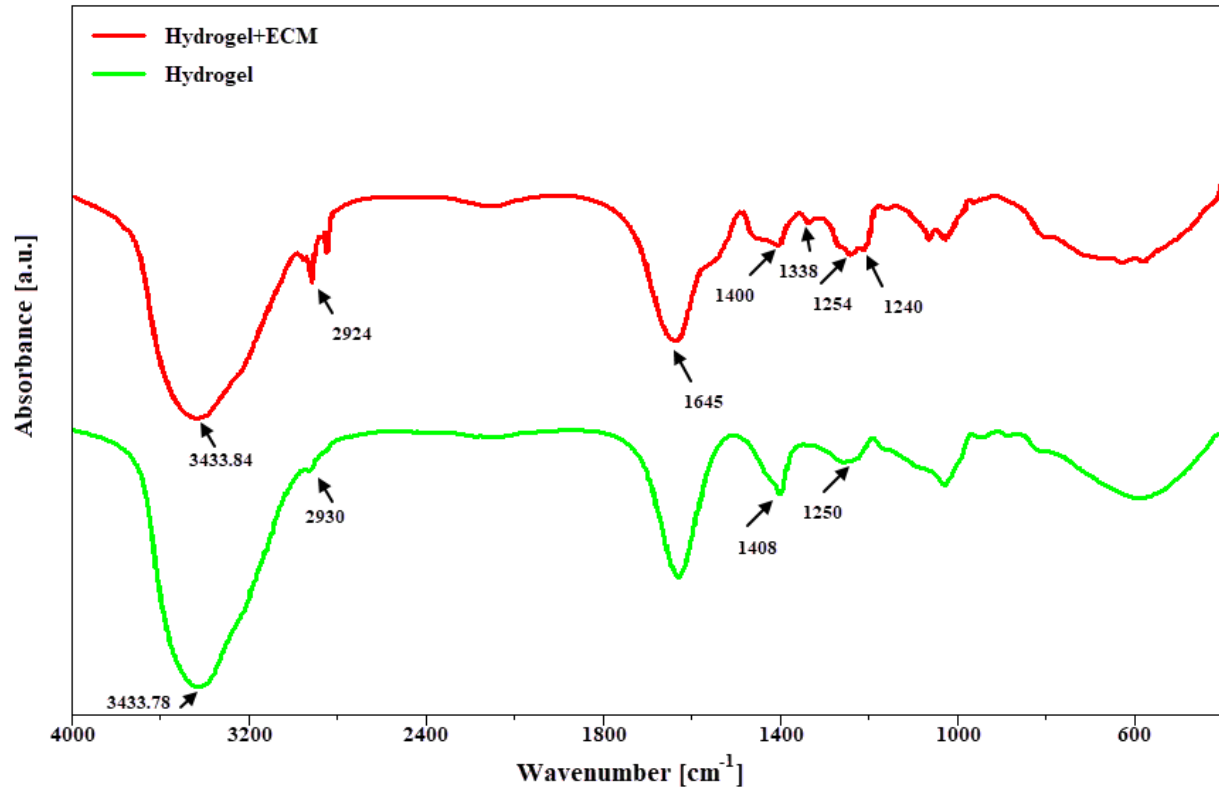


Figure 3. FTIR spectra of hydrogel and hydrogel with 4% w/v ECM.

3.4. Characterization of isolated hASCs

One of the appropriate approaches for cartilage regeneration is using hASCs. Because these multipotent stem cells enable easy harvesting and have a high proliferation rate; also, hASCs can be differentiated into chondrocytes [43]. In this study, to approve the mesenchymal stem cells' quality and assess their potential for differentiation to osteocytes and fat cells, the multi-lined test was utilized. The flow cytometric results confirmed that the cells were positive for mesenchymal CD markers, including CD29 (88.7%), CD90 (98.4%), and CD105 (90.4%) antigens. Further, the cells represented negative for the hematopoietic markers of CD31 (0.219%) and CD34 (0.608%).

3.5. Optimization of ECM concentration

3.5.1. Influence of concentration of ECM on cell viability

Cell viability of encapsulated hASCs within hydrogels containing different concentrations of ECM powder (0-5% w/v) was investigated using the MTT assay for 7 days. As shown in **Figure 4A**, the results of the MTT assay presented that ECM affects the cell viability of hASCs remarkably. On day 7, the metabolic activity of hASCs was increased significantly by enhancing the ECM concentration ($p < 0.05$). Moreover, increasing the ECM concentration from 0% to 5% w/v resulted in higher cell viability, although upon the addition of 5% ECM, the increase in cell viability compared to 4% ECM hydrogel was insignificant. Our results are consistent with the previous study reported by Tsai et al. that confirms cell viability enhanced with increasing ECM concentration [14].

3.5.2. Influence of ECM concentration on mechanical properties

One of the critical features of scaffolds used in cartilage tissue engineering is the resistance versus breakdown under compression stress [44]. As is expected, incorporating ECM powder into the hydrogel improves the compressive strength because ECM acts as a rigid filler [44,45]. The compressive modulus (**Figure 4B**) of the hydrogel, including different concentrations of ECM, demonstrated significant growth by increasing ECM concentrations. In **Figure 4B**, the compressive modulus of the hydrogel at 4% w/v (208 ± 17 kPa) was remarkably higher than those of the hydrogels at 0% w/v (66 ± 5 kPa), 1% w/v (86 ± 1 kPa), 2% w/v (91 ± 4 kPa), 3% w/v (115 ± 3 kPa), and 5% w/v (89 ± 5 kPa) ($p < 0.05$). The compressive modulus of the hydrogel at 2% w/v showed no significant difference from those of the hydrogels at 5% w/v, 3% w/v and 1% w/v, while the hydrogel without ECM demonstrated the lowest compressive modulus ($p < 0.005$). It

was expected to see a high compressive modulus for the hydrogel with 5% ECM; however, it showed a very low mechanical strength, which can be due to the agglomeration of the ECM powders making the structure too crunchy compared to the other hydrogels. Based on similar studies, it can be said that increasing ECM concentration can enhance mechanical properties [14,44], although using the fillers may result in phase separation and failure of the structures [47,48]. Furthermore, alginates have been shown not to provide a good adhesion role due to their chemical structure. In contrast, it has been reported that alginate sulfate causes cell spreading due to having a strong affinity for growth factors and decreased stiffness of the alginate. Hence, using a blend of alginate and sulfate alginate creates a hydrogel with suitable mechanical and biological properties.

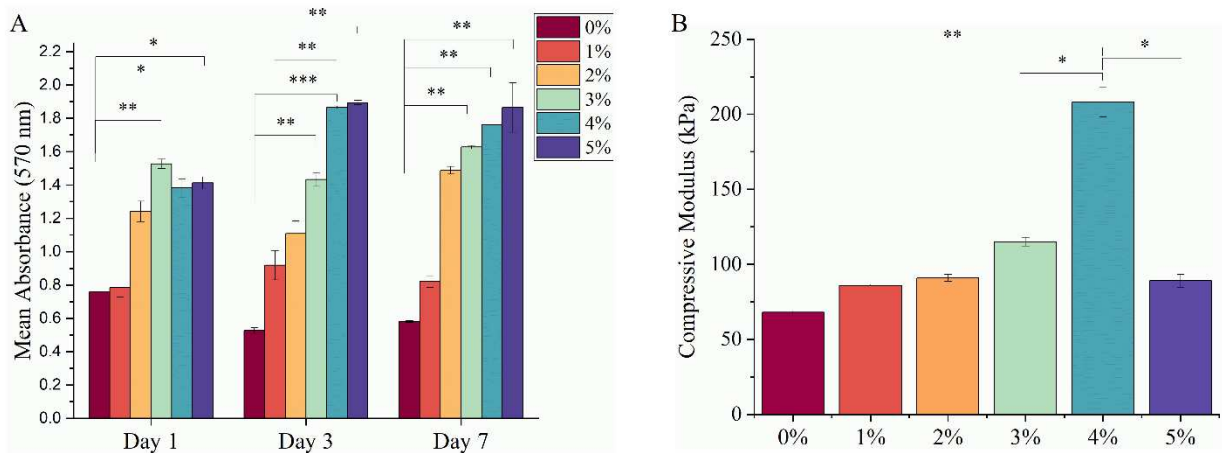


Figure 4. The MTT assay for evaluation of hASCs metabolic activity after 1, 3, and 7 days of cell encapsulation in various concentrations of ECM (A) and the compressive stress of hydrogel containing different concentrations of ECM powder (B) (0%, 1%, 2%, 3%, 4% and 5% w/v) (* $p < 0.05$, ** $p < 0.005$, *** $p < 0.0005$).

3.6. Influence of ECM concentration on rheological properties

To assess the effect of ECM on the rheological properties of the hydrogels, initially, the amplitude (strain) sweep tests at various frequencies were carried out to ensure that the applied strain was within the linear viscoelastic region and was fixed at 0.2% for frequency sweep tests. This measurement was performed at 37 °C in the strain range of 0.01–100%, as shown in **Figure 5A** and **Figure 5B**. Both elastic modulus (G') and loss modulus (G'') showed increasing trends upon the addition of ECM up to 4% compared to the hydrogel without ECM, indicating the ECM incorporated in the hydrogel structure. However, the hydrogel with 5% ECM demonstrated a sensible decrease in the rheological behavior, which can be due to the agglomeration of ECM and its fragile structure. In fact, the addition of ECM caused failure points which can be observed in both compression and shear-based modulus. It is worth mentioning that, in all the hydrogels regardless of the presence of ECM, G' showed higher values in comparison with G'' , indicating that the hydrogels have elastic nature, which is desirable as the intention is to be used in cartilage tissue with the same behavior. The damping factor, which is the ratio between G'' to G' can also be used to show the elastic nature when the values are lower than 1. The concentration of alginate and alginate sulfate, their ratio, crosslinking degree, un-crosslinked sections and ECM content can be directly related to the G' . In another word, samples with higher G' are able to resist greater deformations compared to the samples with lower deformations [46,48]. By adding ECM up to 4%, samples became more elastic; however, as expected, the 5% ECM sample showed lower results due to the agglomeration and fragile structure. Hydrogel with 0%, 1% and 5% ECM illustrated lower values for damping up to around 3% strain, and hydrogel with 2% ECM showed values near 1 up to ~5%, while hydrogels 3% and 4% depicted damping values lower than 1 up to 15% strain.

To further assess the effect of ECM on the rheological behavior of the hydrogels dynamic frequency sweep measurements (**Figure 5C** and **5D**) were carried out. Similar to strain sweep tests, an increasing trend up to 4% ECM was observed in both G' and G'' against frequency, although by loading ECM, the modulus of the samples showed a drastic increase. The main reason for such an increase is that ECM enhances the interaction between alginate and alginate sulfate, which restricts polymer chain movements [46,48]. Generally, when polymer chains are crosslinked, they become longer compared to less crosslinked networks, leading to longer relaxation times [49]. The hydrogel with 0% ECM showed an unstable structure at higher frequencies as there was no ECM to increase the interaction of components, and therefore there was a lower density of crosslinks in this hydrogel. The elastic properties dominate all the samples containing ECM since the rate of increase of G' ($\Delta G'/\Delta t$) was higher than G'' . Moreover, frequency sweep results illustrated no intersection between the modulus, indicating that the addition of ECM and crosslinking, both at the same time, enhanced the molecular weight and polymer chains need more time for deformation. In other words, the transition from the mostly viscous regime to the mostly elastic regime happens over longer times, lower frequencies, and lower stresses [50]. The complex viscosity of the samples (**Figure 5F**) also increased by adding ECM up to 4% due to a better network formation as the ECM caused better interactions between the hydrogel components.

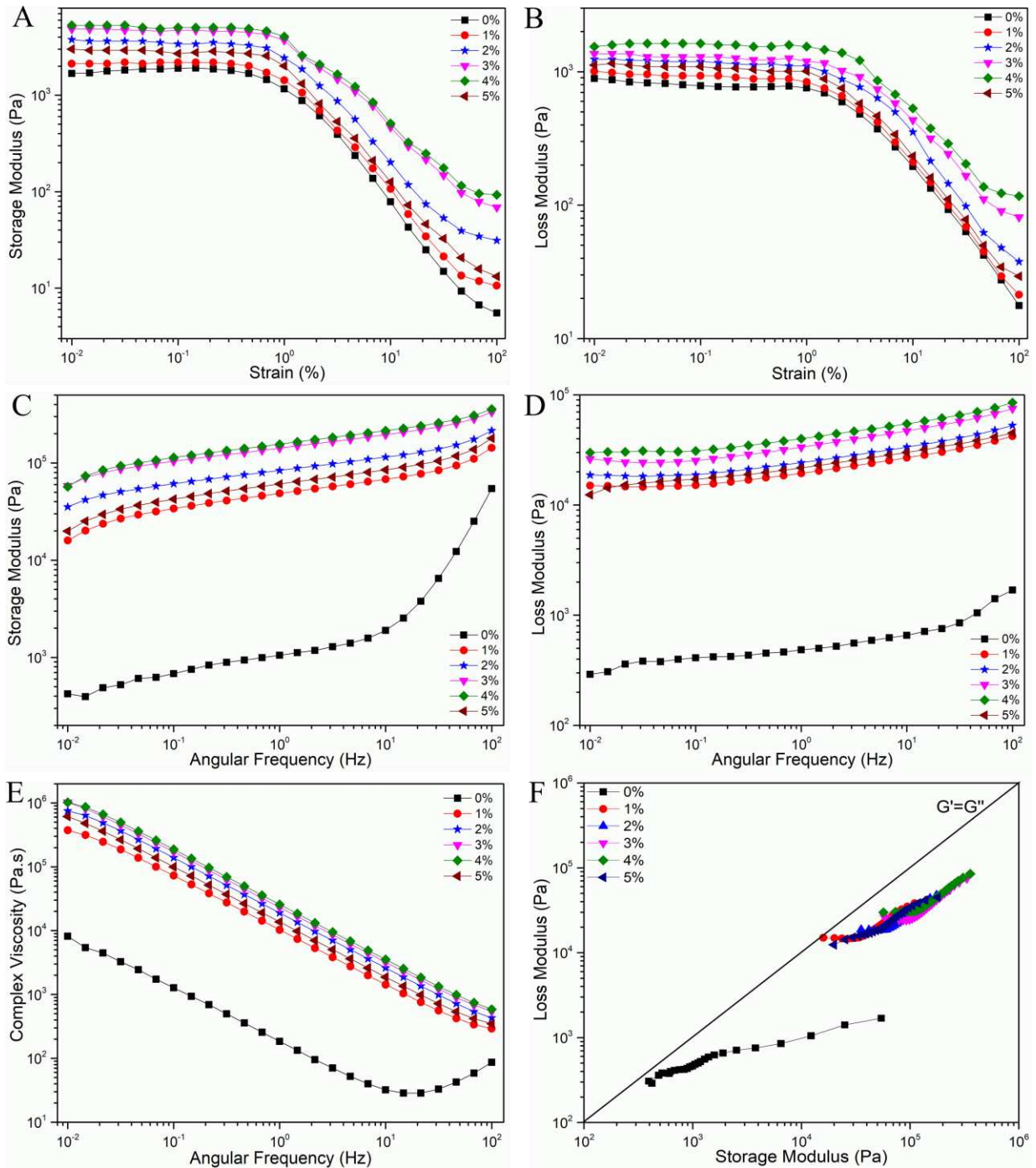


Figure 5. Rheological properties of selected hydrogels, including the (a,b) strain sweep (c,d,e) frequency sweep (f) Cole-Cole modified curves.

In order to further confirm the elastic nature of the hydrogels and their structural diversity at 37 °C, modified Cole-Cole curves were used, which are a logarithmic plot of G'' versus G' (**Figure 5E**). The equi-modulus $G'=G''$ line is also presented in the plot, and crossing this line shows a change in the viscoelastic behavior [46,50,51]. According to this curve, none of the hydrogels crossed the line, indicating a complete elastic behavior. The addition of ECM shifted the modulus to the higher values and imposed a more elastic nature on them; therefore, the relaxation time of hydrogels with ECM was longer (τ) in comparison with the hydrogel without ECM.

The cell viability, mechanical and rheological results depicted that the 4% w/v group can increase cell survival and support cell growth by providing a suitable and stable substrate; thus, 4% w/v of ECM powder was selected as the optimum.

3.7. Optimization of the layered hydrogel-nanofiber composite structure

3.7.1. Water retention ability

To evaluate the influence of the number of layers on the water retention ability of prepared composites, the swelling ratio of composites with different layers (2-layer, 3-layer, and 5-layer) was examined and is shown in **Figure 6A**. The results demonstrated that the swelling ratio of the hydrogel ($291 \pm 14\%$) was higher than the 5-layer ($212 \pm 18\%$), 2-layer ($200.33 \pm 8\%$), and 3-layer ($191 \pm 10\%$). It can be related to the improved interaction between electrospun nanofibers and hydrogel networks, which results in higher crosslinking and can decrease the swelling ratio [43]. The swelling ratio for the 5-layer had an increase in comparison with 2 and 3-layer because of the presence of two layers of hydrogel in the composite.

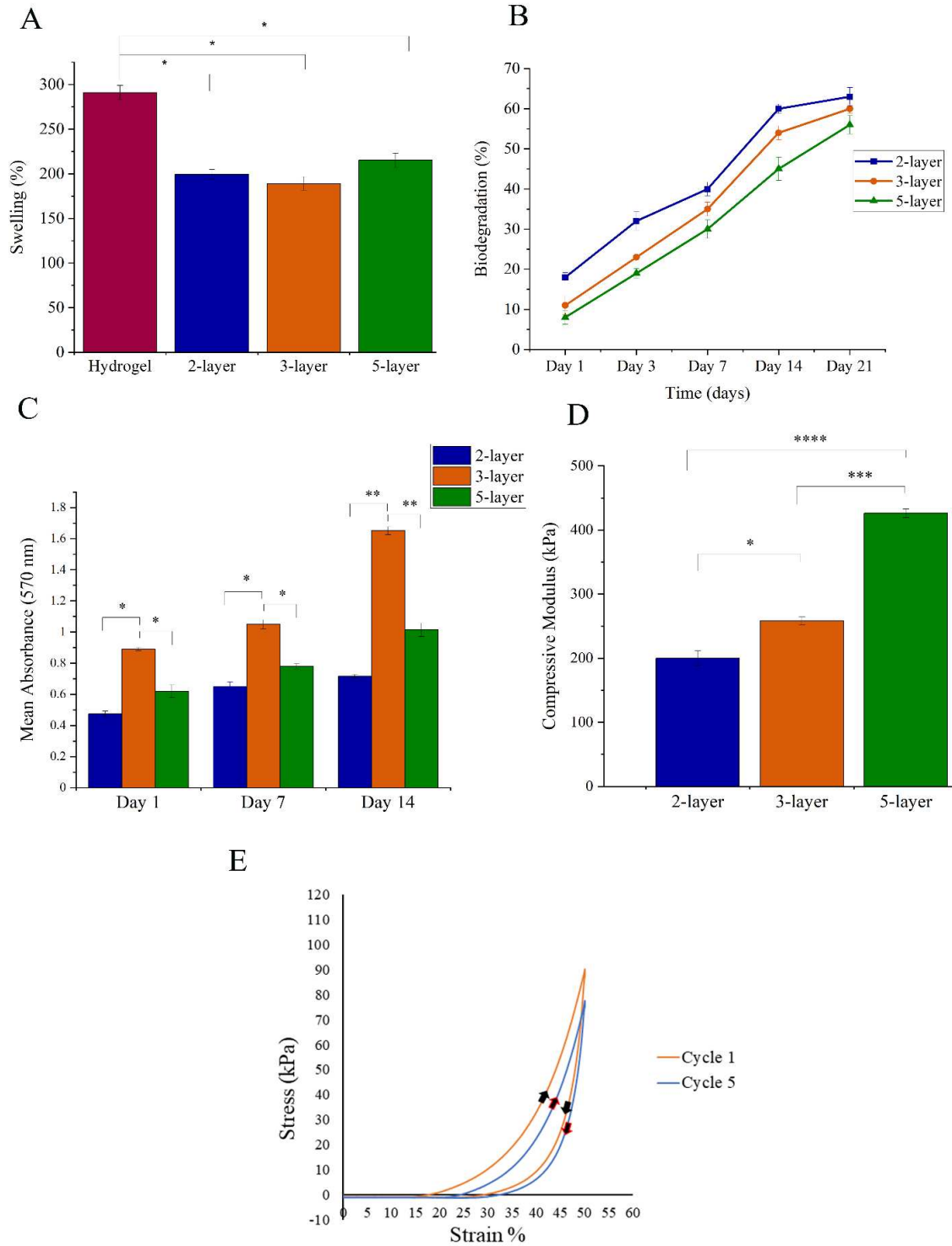


Figure 6. The swelling ratio of hydrogel (control) and composite with different layers (2-layer, 3-layer, and 5-layer) (A), the degradation rate of hydrogel and composite with different layers (2-layer, 3-layer, and 5-layer) within 21 days (B), the MTT assay for evaluation metabolic activity of

encapsulated hASCs within the sandwich constructs containing different layers of nanofibers (2-layer, 3-layer, and 5-layer) after 1, 7, and 14 days (C), the compressive stress of the sandwich constructs (2-layer, 3-layer, and 5-layer) (D) and 10 cyclic compressive fatigue tests for the 3-layer or optimal scaffold (E) (*p < 0.05, **p < 0.005, ***).

3.7.2. Degradation behavior

The effects of the number of composite layers on biodegradation were assessed by the weight loss of the composite with various layers within 21 days, given in **Figure 6B**. All samples were degraded over time with several ratios because of different factors. For example, alginate/alginate sulfate has a variety of degradation rates due to the degree of crosslinking and molecular weight. Variety rates of degradation are helpful to develop a suitable design for cell encapsulation and allow the native ECM of cells to replace hydrogel [53]. By immersing alginate/alginate sulfate hydrogel in PBS, ion exchange between hydrogel and PBS buffer causes degradation [54]. As shown in **Figure 6B**, the degradation rate in the early days represented higher amounts, although it decreased over time due to the decline of the ion exchange rate. However, there was a direct relation between less biodegradation and the number of layers of electrospun nanofibers; the degradation rate decreased by increasing the number of layers [43]. In the initial days, all the composites due to gelatin release from electrospun nanofibers and high ion exchange from hydrogel had greater degradation rates, which within the time faced a noticeable decrement.

3.7.3. Investigating the cell viability

The effect of the number of layers of hydrogel-nanofiber constructs on the cell viability of encapsulated hASCs within the hydrogel layer of composite was investigated through the MTT

assay over 14 days. As shown in **Figure 6C**, the results of the MTT assay represented that on day 14, the metabolic activity of hASCs significantly increased by adding layers from 2-layer to 3-layer and decreased from 3-layer to 5-layer ($p < 0.05$). Also, the results of day 1 and day 7 confirmed the obtained trend. This result can be related to improving cell spreading by increasing the number of layers from double to 3-layer since mechanical properties enhance. The nanofiber layers in the sandwich constructs result in a betterment of mimicking available collagen in the ECM structure, which leads to higher mechanical properties that promote cell proliferation and differentiation [54,55]. In a similar study, by encapsulating hASCs within sandwich constructs (PCL/methacrylated GT), it has been shown that cell metabolism was enhanced; however, it did not improve cell proliferation [31]. Cell spreading can be inhibited by increasing the number of layers from 3-layer to 5-layer due to the slower cell diffusion.

3.7.4. Influence of composition on mechanical properties

Unconfined compressive strength was performed to evaluate how the number of layers affects the mechanical properties of the composite. The compressive modulus (**Figure 6D**) of the sandwich constructs demonstrated an upward trend with increasing the number of layers. As can be seen in **Figure 6D**, the compressive modulus of the 5-layer (426 ± 12 kPa) was significantly more than those of the 2-layer (200 ± 20 kPa) and 3-layer (258 ± 11 kPa) ($p < 0.05$). The added PCL-GT layer to the structure enhances the compressive modulus due to the compressive stress transmitted on the surface of the fibers, hydrogels, and their interface [43]. There are four articular cartilage zones with different mechanical properties: superficial zone, middle zone, deep zone, and calcified cartilage that have compressive Young's Modulus between 240–850 kPa [57]; therefore, the composite structures containing 3 and 5-layer are suitable for cartilage tissue engineering.

According to the MTT assay results, mechanical test, swelling, and biodegradation analysis, the 3-layer scaffold was selected as the optimum scaffold for further investigations.

The cyclic compressive experiment was conducted in the compressive fracturing in **Figure 6E**. The stress/strain curve shows a classic viscoelastic behavior, identified by the non-linear increase of stress with increasing strain. 3-layers composite with a compressive strain of 50% was conducted for 5 loading/unloading cycles. The stress–strain curves contained a linear region at initial strains of less than 20% and a region with an increasing slope at strains of 25–50%. With the increase of cyclic compressive load from one to 5 times, the compression set of the composite increased slightly, and the compression was still able to maintain high strength and structural integrity. After 5 times compressions, hydrogels could quickly restore the original state and maintain 90% of the original stress at 50% strain.

3.8. The influence of hydrogel-nanofiber scaffold containing ECM on chondrogenic-like differentiation of hASCs

Chondrogenic-like differentiation of hASCs was investigated using Alcian Blue staining after 21 days of culture (**Figure 7**). The hydrogel with chondrogenesis media was used as the negative control. The scaffold is shown in purple in **Figure 7 A-C**, whereas the region where ECM synthesis occurs is shown in blue. The results demonstrated that hASCs within the scaffold containing ECM powder synthesized more glycosaminoglycans than encapsulated hASCs in the scaffold without ECM. Therefore, it can be concluded that a composite containing ECM powder represents an appropriate capability to differentiate.

3.9. Real-time PCR

The chondrogenic differentiation and expression of chondrocyte markers (collagen II (COL II), SRY-Box Transcription Factor 9 (SOX 9), Aggrecan (ACAN)) of encapsulated hASCs

within the hydrogel layer of the composite were investigated through real-time PCR over 14 days. As shown in **Figure 7 D-F**, the results of real-time PCR represented that on day 14, the expression level of SOX9, ACAN, and COL II was significantly increased by adding PCL/GT layers and ECM powder to the hydrogel. The results of real-time PCR demonstrated that ECM powder and PCL/GT layers enhanced mechanical and biological behavior governed by cartilage markers expression by hASCs.

As can be seen in **Figure 7 D-F**, the expression level of SOX9, ACAN, and COL II of the composite with ECM powder was significantly more than those of the composite without ECM powder and hydrogel ($p < 0.0005$). SOX9 is one of the main genes in developing adult cartilage and an active gene throughout chondrocyte differentiation. The high-level expression can enhance the expression level of cartilage-related genes like collagen type II and aggrecan [57–59]. As shown, the target group in this study has the highest expression of SOX9. The main group also has the highest expression levels of collagen type II and aggrecan.

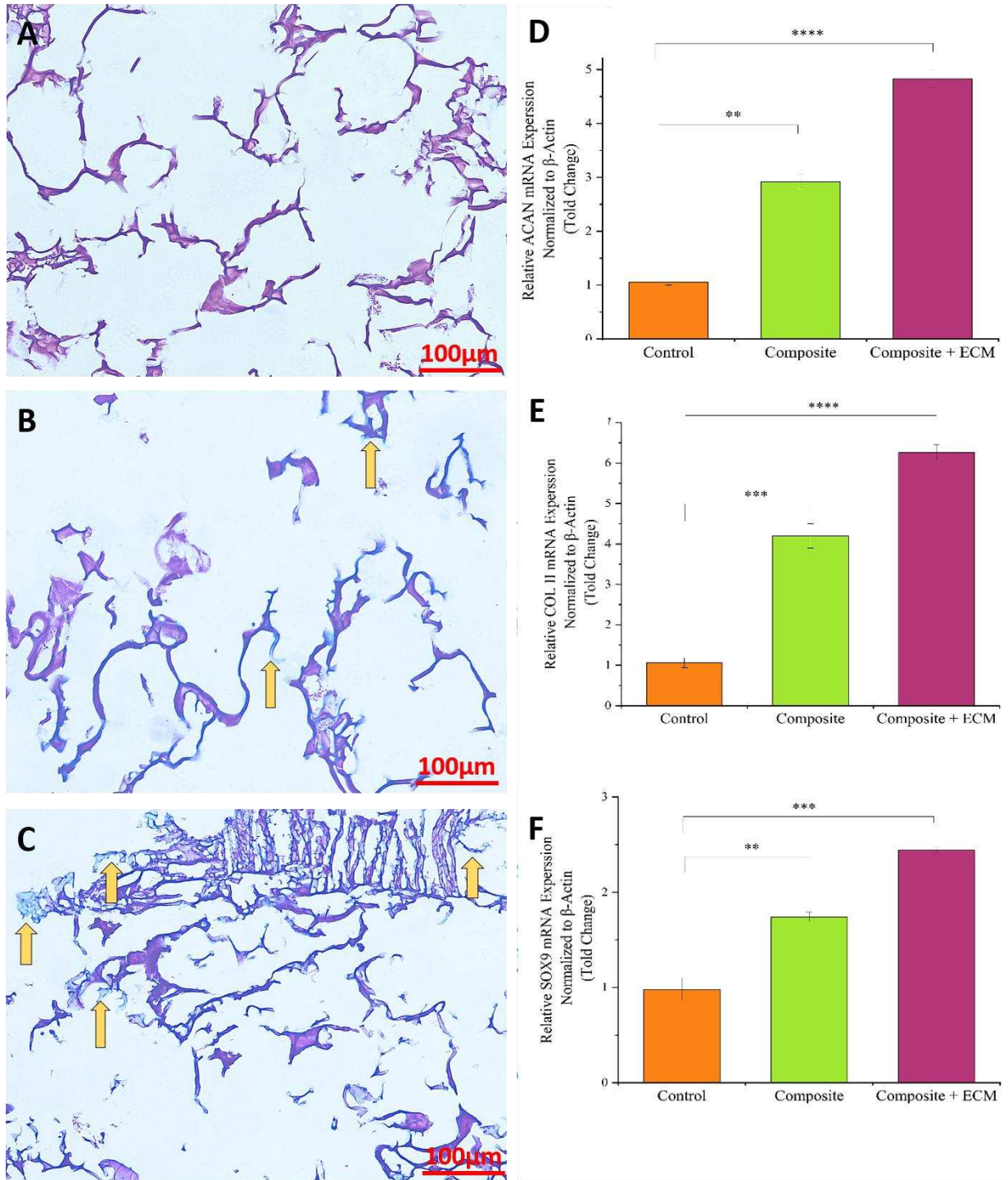


Figure 7. Hydrogel (Control) (A), the scaffold without ECM powder (Composite) (B), and the 3-layer sandwich-like scaffold containing ECM powder (Composite + ECM) (C) were stained by Alcian Blue after 21 days. **Arrows point to the ECM expression.** Evaluation of chondrogenic

differentiation by real-time PCR for 3-layer composite scaffold with and without ECM. The control group (hydrogel) was selected as a reference group, and the mRNA levels were normalized to 1, ACAN (D), COL II (E), and SOX9 (F) (*p < 0.05, **p < 0.005, ***p < 0.0005. ****p < 0.0005).

Conclusion

This study developed a promising composite scaffold containing ECM powder and several layers of hydrogel and nanofibers, which can mimic cartilage structure and characteristics. The addition of ECM powder resulted in different properties, such as enhanced mechanical strength and cell proliferation and improved chondrogenic differentiation noticeably. Also, the MTT assay demonstrated that adding layers of electrospun nanofibers to the hydrogel improves cell spreading by increasing the number of layers from 2 to 3-layer since mechanical properties are enhanced. Furthermore, enhanced chondrogenic-like differentiation of hASCs in composite compared to the control group illustrates their concrete potential for more studies accompanied by the significant application of cartilage tissue engineering.

Declarations of interest

None

References

- [1] Z. H. Deng, Y. S. Li, X. Gao, G. H. Lei, and J. Huard, “Bone morphogenetic proteins for articular cartilage regeneration,” *Osteoarthr. Cartil.*, vol. 26, no. 9, pp. 1153–1161, 2018, doi: 10.1016/j.joca.2018.03.007.
- [2] Y. Krishnan and A. J. Grodzinsky, “Cartilage diseases,” *Matrix Biol.*, vol. 71–72, no. 2017, pp. 51–69, 2018, doi: 10.1016/j.matbio.2018.05.005.
- [3] A. Mellati *et al.*, “Microengineered 3D cell-laden thermoresponsive hydrogels for mimicking cell morphology and orientation in cartilage tissue engineering,” *Biotechnol. Bioeng.*, vol. 114, no. 1, pp. 217–231, 2017, doi: 10.1002/bit.26061.
- [4] F. Mohabatpour, A. Karkhaneh, and A. M. Sharifi, “A hydrogel/fiber composite scaffold for chondrocyte encapsulation in cartilage tissue regeneration,” *RSC Adv.*, vol. 6, no. 86, pp. 83135–83145, 2016, doi: 10.1039/c6ra15592h.
- [5] C. Wang *et al.*, “Injectable Cholesterol-Enhanced Stereocomplex Polylactide Thermogel Loading Chondrocytes for Optimized Cartilage Regeneration,” *Adv. Healthc. Mater.*, vol. 8, no. 14, pp. 1–10, 2019, doi: 10.1002/adhm.201900312.
- [6] H. Le, W. Xu, X. Zhuang, F. Chang, Y. Wang, and J. Ding, “Mesenchymal stem cells for cartilage regeneration,” *J. Tissue Eng.*, vol. 11, 2020, doi: 10.1177/2041731420943839.
- [7] M. Zayed, S. Adair, T. Ursini, J. Schumacher, N. Misk, and M. Dhar, “Concepts and challenges in the use of mesenchymal stem cells as a treatment for cartilage damage in the horse,” *Res. Vet. Sci.*, vol. 118, pp. 317–323, 2018, doi: 10.1016/j.rvsc.2018.03.011.
- [8] M. Aleemardani *et al.*, “Can Tissue Engineering Bring Hope to the Development of Human Tympanic Membrane?,” *Tissue Engineering Part B: Reviews*. 2021, doi: 10.1089/ten.teb.2020.0176.
- [9] B. S. Kim *et al.*, “Design of artificial extracellular matrices for tissue engineering,” *Prog. Polym. Sci.*, vol. 36, no. 2, pp. 238–268, 2011, doi: 10.1016/j.progpolymsci.2010.10.001.
- [10] P. Gir, G. Oni, S. A. Brown, A. Mojallal, and R. J. Rohrich, “Human adipose stem cells: Current clinical applications,” *Plast. Reconstr. Surg.*, vol. 129, no. 6, pp. 1277–1290, 2012, doi: 10.1097/PRS.0b013e31824eca66.
- [11] M. Locke, J. Windsor, and P. R. Dunbar, “Human adipose-derived stem cells: Isolation, characterization and applications in surgery,” *ANZ J. Surg.*, vol. 79, no. 4, pp. 235–244, 2009, doi: 10.1111/j.1445-2197.2009.04852.x.
- [12] P. Palumbo, F. Lombardi, G. Siragusa, M. G. Cifone, B. Cinque, and M. Giuliani, “Methods of isolation, characterization and expansion of human adipose-derived stem cells (ASCs): An overview,” *Int. J. Mol. Sci.*, vol. 19, no. 7, 2018, doi:

10.3390/ijms19071897.

- [13] G. BORCHARDT, “Chapter 14 Chapter 14,” *LR Lloyd’s Regist.*, vol. 100, no. July, pp. 1–35, 1989, doi: 10.1007/978-1-61737-960-4.
- [14] C. Tsai, S. Kuo, T. Lu, N. Cheng, M. Shie, and J. Yu, “Enzyme-Cross-linked Gelatin Hydrogel Enriched with an Articular Cartilage Extracellular Matrix and Human Adipose-Derived Stem Cells for Hyaline Cartilage Regeneration of Rabbits,” 2020, doi: 10.1021/acsbiomaterials.9b01756.
- [15] L. Edgar *et al.*, “Utility of extracellular matrix powders in tissue engineering,” *Organogenesis*, vol. 14, no. 4, pp. 172–186, 2018, doi: 10.1080/15476278.2018.1503771.
- [16] “1,2 †,” doi: 10.1002/term.2465.
- [17] H. J. Oh, S. H. Kim, J. H. Cho, S. H. Park, and B. H. Min, “Mechanically Reinforced Extracellular Matrix Scaffold for Application of Cartilage Tissue Engineering,” *Tissue Eng. Regen. Med.*, vol. 15, no. 3, pp. 287–299, 2018, doi: 10.1007/s13770-018-0114-1.
- [18] Y. Han, X. Li, Y. Zhang, Y. Han, F. Chang, and J. Ding, “Mesenchymal stem cells for regenerative medicine,” *Cells*, vol. 8, no. 8, 2019, doi: 10.3390/cells8080886.
- [19] D. Puppi, F. Chiellini, A. M. Piras, and E. Chiellini, “Polymeric materials for bone and cartilage repair,” *Prog. Polym. Sci.*, vol. 35, no. 4, pp. 403–440, 2010, doi: 10.1016/j.progpolymsci.2010.01.006.
- [20] B. Roushangar Zineh, M. R. Shabgard, and L. Roshangar, “Mechanical and biological performance of printed alginate/methylcellulose/halloysite nanotube/polyvinylidene fluoride bio-scaffolds,” *Mater. Sci. Eng. C*, vol. 92, no. July, pp. 779–789, 2018, doi: 10.1016/j.msec.2018.07.035.
- [21] A. Sionkowska, “Current research on the blends of natural and synthetic polymers as new biomaterials: Review,” *Prog. Polym. Sci.*, vol. 36, no. 9, pp. 1254–1276, 2011, doi: 10.1016/j.progpolymsci.2011.05.003.
- [22] A. Anindyajati, “Electrospun Biomaterials and Related Technologies,” *J. Teknosains*, vol. 8, no. 2, p. 168, 2019, doi: 10.22146/teknosains.46652.
- [23] A. Cipitria, A. Skelton, T. R. Dargaville, P. D. Dalton, and D. W. Hutmacher, “Design, fabrication and characterization of PCL electrospun scaffolds - A review,” *J. Mater. Chem.*, vol. 21, no. 26, pp. 9419–9453, 2011, doi: 10.1039/c0jm04502k.
- [24] “13.pdf.” .
- [25] R. Zheng *et al.*, “The influence of Gelatin/PCL ratio and 3-D construct shape of electrospun membranes on cartilage regeneration,” *Biomaterials*, vol. 35, no. 1, pp. 152–164, 2014, doi: 10.1016/j.biomaterials.2013.09.082.

- [26] M. Szekalska, A. Puciłowska, E. Szymańska, P. Ciosek, and K. Winnicka, “Alginate: Current Use and Future Perspectives in Pharmaceutical and Biomedical Applications,” *Int. J. Polym. Sci.*, vol. 2016, 2016, doi: 10.1155/2016/7697031.
- [27] Z. Zhang, O. Ortiz, R. Goyal, and J. Kohn, *Biodegradable Polymers*. Elsevier Inc., 2014.
- [28] Ø. Arlov and G. Skjåk-Bræk, “Sulfated alginates as heparin analogues: A review of chemical and functional properties,” *Molecules*, vol. 22, no. 5, pp. 1–16, 2017, doi: 10.3390/molecules22050778.
- [29] L. Daelemans, I. Steyaert, E. Schoolaert, C. Goudenhoft, H. Rahier, and K. De Clerck, “Nanostructured hydrogels by blend electrospinning of polycaprolactone/gelatin nanofibers,” *Nanomaterials*, vol. 8, no. 7, pp. 1–12, 2018, doi: 10.3390/nano8070551.
- [30] S. Karimi, Z. Bagher, N. Najmoddin, S. Simorgh, and M. Pezeshki-Modaress, “Alginate-magnetic short nanofibers 3D composite hydrogel enhances the encapsulated human olfactory mucosa stem cells bioactivity for potential nerve regeneration application,” *Int. J. Biol. Macromol.*, vol. 167, pp. 796–806, 2021, doi: 10.1016/j.ijbiomac.2020.11.199.
- [31] G. Yang, H. Lin, B. B. Rothrauff, S. Yu, and R. S. Tuan, “Multilayered polycaprolactone/gelatin fiber-hydrogel composite for tendon tissue engineering,” *Acta Biomater.*, vol. 35, pp. 68–76, 2016, doi: 10.1016/j.actbio.2016.03.004.
- [32] S. Simorgh *et al.*, “Human olfactory mucosa stem cells delivery using a collagen hydrogel: As a potential candidate for bone tissue engineering,” *Materials (Basel)*, vol. 14, no. 14, pp. 1–17, 2021, doi: 10.3390/ma14143909.
- [33] M. Aleemardani, A. Solouk, S. Akbari, and M. Mehdi, “Materialia Silk-derived oxygen-generating electrospun patches for enhancing tissue regeneration : Investigation of calcium peroxide role and its effects on controlled oxygen delivery,” *Materialia*, vol. 14, no. April, p. 100877, 2020, doi: 10.1016/j.mtla.2020.100877.
- [34] A. Sadeghi, M. Zandi, M. Pezeshki-modaress, and S. Rajabi, “International Journal of Biological Macromolecules Tough , hybrid chondroitin sulfate nano fi bers as a promising scaffold for skin tissue engineering,” *Int. J. Biol. Macromol.*, vol. 132, pp. 63–75, 2019, doi: 10.1016/j.ijbiomac.2019.03.208.
- [35] S. Bagheri *et al.*, “Control of cellular adhesiveness in hyaluronic acid-based hydrogel through varying degrees of phenol moiety cross-linking,” *J. Biomed. Mater. Res. - Part A*, vol. 109, no. 5, pp. 649–658, 2021, doi: 10.1002/jbm.a.37049.
- [36] A. Hivechi *et al.*, “Cellulose nanocrystal effect on crystallization kinetics and biological properties of electrospun polycaprolactone,” *Mater. Sci. Eng. C*, vol. 121, no. January, p. 111855, 2021, doi: 10.1016/j.msec.2020.111855.
- [37] M. A. Villar-fernandez, J. A. Lopez-escamez, N. G. Cts, and C. Genomics, “Outlook for tissue engineering of the tympanic membrane on co m m e r c i u s e o n o n e r a l,” vol. 5, pp.

- 9–19, 2015, doi: 10.4081/audiores.2015.117.
- [38] J. Li *et al.*, “p38 MAPK mediated in compressive stress-induced chondrogenesis of rat bone marrow MSCs in 3D alginate scaffolds,” *J. Cell. Physiol.*, vol. 221, no. 3, pp. 609–617, 2009, doi: 10.1002/jcp.21890.
- [39] H. Samadian *et al.*, “Sophisticated polycaprolactone/gelatin nanofibrous nerve guided conduit containing platelet-rich plasma and citicoline for peripheral nerve regeneration: In vitro and in vivo study,” *Int. J. Biol. Macromol.*, vol. 150, pp. 380–388, 2020, doi: 10.1016/j.ijbiomac.2020.02.102.
- [40] C. R. Badita, D. Aranghel, C. Burducea, and P. Mereuta, “Characterization of sodium alginate based films,” *Rom. J. Phys.*, vol. 65, no. 1–2, pp. 1–8, 2020.
- [41] I. Freeman, A. Kedem, and S. Cohen, “The effect of sulfation of alginate hydrogels on the specific binding and controlled release of heparin-binding proteins,” *Biomaterials*, vol. 29, no. 22, pp. 3260–3268, 2008, doi: 10.1016/j.biomaterials.2008.04.025.
- [42] A. Manuscript, “pt,” 2020.
- [43] P. Zare *et al.*, “Alginate sulfate-based hydrogel/nanofiber composite scaffold with controlled Kartogenin delivery for tissue engineering,” *Carbohydr. Polym.*, vol. 266, p. 118123, Apr. 2021, doi: 10.1016/j.carbpol.2021.118123.
- [44] Y. Zhang and P. Habibovic, “Delivering Mechanical Stimulation to Cells: State of the Art in Materials and Devices Design,” *Adv. Mater.*, vol. 34, no. 32, 2022, doi: 10.1002/adma.202110267.
- [45] J. Wu, Q. Ding, A. Dutta, Y. Wang, Y. Huang, and H. Weng, “Acta Biomaterialia An injectable extracellular matrix derived hydrogel for meniscus repair and regeneration,” *ACTA Biomater.*, no. February, 2015, doi: 10.1016/j.actbio.2015.01.027.
- [46] S. Utech and A. R. Boccaccini, *A review of hydrogel-based composites for biomedical applications: enhancement of hydrogel properties by addition of rigid inorganic fillers*, vol. 51, no. 1. Springer US, 2016.
- [47] S. Saeedi Garakani *et al.*, “Fabrication of chitosan/agarose scaffolds containing extracellular matrix for tissue engineering applications,” *Int. J. Biol. Macromol.*, vol. 143, pp. 533–545, 2020, doi: 10.1016/j.ijbiomac.2019.12.040.
- [48] P. Zare *et al.*, “An additive manufacturing-based 3D printed poly ϵ -caprolactone/alginate sulfate/extracellular matrix construct for nasal cartilage regeneration,” *J. Biomed. Mater. Res. - Part A*, vol. 110, no. 6, pp. 1199–1209, 2022, doi: 10.1002/jbm.a.37363.
- [49] Z. Mousavi Nejad *et al.*, “Synthesis, physicochemical, rheological and in-vitro characterization of double-crosslinked hyaluronic acid hydrogels containing dexamethasone and PLGA/dexamethasone nanoparticles as hybrid systems for specific

- medical applications,” *Int. J. Biol. Macromol.*, vol. 126, pp. 193–208, 2019, doi: 10.1016/j.ijbiomac.2018.12.181.
- [50] S. J. Falcone, D. M. Palmeri, and R. A. Berg, “Rheological and cohesive properties of hyaluronic acid,” *J. Biomed. Mater. Res. - Part A*, vol. 76, no. 4, pp. 721–728, 2006, doi: 10.1002/jbm.a.30623.
- [51] S. M. Davachi, B. S. Heidari, R. Sahraeian, and A. Abbaspourrad, “The effect of nanoperlite and its silane treatment on the crystallinity, rheological, optical, and surface properties of polypropylene/nanoperlite nanocomposite films,” *Compos. Part B Eng.*, vol. 175, no. November 2018, p. 107088, 2019, doi: 10.1016/j.compositesb.2019.107088.
- [52] R. Sahraeian, S. M. Davachi, and B. S. Heidari, “The effect of nanoperlite and its silane treatment on thermal properties and degradation of polypropylene/nanoperlite nanocomposite films,” *Compos. Part B Eng.*, vol. 162, pp. 103–111, 2019, doi: 10.1016/j.compositesb.2018.10.093.
- [53] G. D. Nicodemus and S. J. Bryant, “Cell encapsulation in biodegradable hydrogels for tissue engineering applications,” *Tissue Eng. - Part B Rev.*, vol. 14, no. 2, pp. 149–165, 2008, doi: 10.1089/ten.teb.2007.0332.
- [54] N. C. Hunt, A. M. Smith, U. Gbureck, R. M. Shelton, and L. M. Grover, “Encapsulation of fibroblasts causes accelerated alginate hydrogel degradation,” *Acta Biomater.*, vol. 6, no. 9, pp. 3649–3656, 2010, doi: 10.1016/j.actbio.2010.03.026.
- [55] J. Jang, H. Oh, J. Lee, T. H. Song, Y. Hun Jeong, and D. W. Cho, “A cell-laden nanofiber/hydrogel composite structure with tough-soft mechanical property,” *Appl. Phys. Lett.*, vol. 102, no. 21, 2013, doi: 10.1063/1.4808082.
- [56] D. Kai, M. P. Prabhakaran, B. Stahl, M. Eblenkamp, E. Wintermantel, and S. Ramakrishna, “Mechanical properties and in vitro behavior of nanofiberhydrogel composites for tissue engineering applications,” *Nanotechnology*, vol. 23, no. 9, 2012, doi: 10.1088/0957-4484/23/9/095705.
- [57] C. J. Little, N. K. Bawolin, and X. Chen, “Mechanical properties of natural cartilage and tissue-engineered constructs,” *Tissue Eng. - Part B Rev.*, vol. 17, no. 4, pp. 213–227, 2011, doi: 10.1089/ten.teb.2010.0572.
- [58] T. E. Hardingham, R. A. Oldershaw, and S. R. Tew, “Cartilage, SOX9 and Notch signals in chondrogenesis,” *J. Anat.*, vol. 209, no. 4, pp. 469–480, 2006, doi: 10.1111/j.1469-7580.2006.00630.x.
- [59] M. Kadaja *et al.*, “SOX9: A stem cell transcriptional regulator of secreted niche signaling factors,” *Genes Dev.*, vol. 28, no. 4, pp. 328–341, 2014, doi: 10.1101/gad.233247.113.
- [60] V. Lefebvre and M. Dvir-Ginzberg, “SOX9 and the many facets of its regulation in the chondrocyte lineage,” *Connect. Tissue Res.*, vol. 58, no. 1, pp. 2–14, 2017, doi:

10.1080/03008207.2016.1183667.